Bull. Mater. Sci., Vol. 27, No. 4, August 2004, pp. 341–345. © Indian Academy of Sciences.

Corrosion behaviour, microstructure and phase transitions of Zn-based alloys

A K YILDIZ* and M KAPLAN†

Department of Physics, Faculty of Science & Arts, †Department of Metallurgy, Faculty of Technical Education, Firat University, 23169 Elazig, Turkey

MS received 1 August 2003; revised 2 June 2004

Abstract. This paper is aimed at investigating the corrosion behaviour, microstructure and phase transitions of Zn-based alloys with different compositions. The corrosion tests are carried out both in acidic medium using 1 N HCl solution and in temperature dependence of thermogravimetric analysis (TGA). In the two different media, in particular, the corrosion behaviour of Zn-based alloys with respect to Al and Si contents is examined, and microstructure in acidic and TGA and phase transformations in TGA are also studied. Corrosion mechanism in TGA is also examined in terms of oxidation parameters and activation energies. The study reveals that corrosion behaviour of Zn-based alloys in acidic medium shows sometimes an increase and sometimes a decrease with time due to Al content which assists in delaying the corrosion by forming a oxide layer on the surface of Zn-based alloys. This property does not appear in temperature dependence of TGA. Further, Si content appears to remain in main matrix without being affected by acidic solution. On the other hand, it is observed that in microstructure, $AlO(Al_2O_3)$, ZnO oxides and Zn–Cu phase precipitations are formed in main matrix, grain boundaries and partially inside the grains.

Keywords. Zinc-based alloys; weight loss; acidic corrosion; thermogravimetric analysis.

1. Introduction

It has been reported that Zn–Al family of alloys among Zn-based foundry alloys have been used increasingly in past decades (Seah *et al* 1997; Sharma *et al* 1997; Prasad 2000a). In particular, Zn–Al alloys have been used widely in industry because of their excellent fluidity, costability and good mechanical properties as stated by Sharma *et al* (1997). It is also known that Zn–Al alloys consisting of high Zn content have a duplex structure with two phases at 350–400°C temperature outside eutectoid region as can be seen on their phase diagram. Moreover, these alloys consisting of compositions such as Cu, Mg and Si with small amounts of Cd, Sn and Pb have many advantages such as high strength with a low casting temperature. On the other hand, although these alloys can easily be annealed, welding and soldering properties are not so good due to their limited extension properties (Dellis *et al* 1991; Zhu and Islas 1997; Zhu *et al* 1999).

The corrosion behaviour and microstructures of a material are sensitive to the various environments that the material encounters for a particular purpose as reported in various studies done for different materials (Pohlman 1978; Toldin *et al* 1981; Aylor and Moran 1985; Fontana 1987; Colin *et al* 1999; Prasad 2000b; Li 2001; Sharma *et al* 2001). However, not much information is available on the corrosion behaviour of Zn-based alloys. It is also appreciated that the corrosion behaviour of Zn–Al alloys, as it is true for any alloy, is associated with various factors such as microstructure, composition of alloy, production techniques adopted for preparing the contents, etc and that even a very small change in one of these factors can seriously affect corrosion behaviour of the material (Zhu and Islas 1997). Hence, this lead to the argument that the field of corrosion behaviour as well as microstructure and phase transitions of Zn-based alloys with different compositions still remains open for investigation for various purposes in industry.

In view of this, we have produced a Zn-based alloy consisting of several compositions such as Al, Cu, Si and Sn, and aimed to investigate corrosion behaviour depending both on HCl acidic solution using the conventional weight loss method and on temperature using TGA technique. The microstructure and phase transitions of the alloy are also investigated.

2. Experimental

Zn-based ingot casting alloy was prepared from high purity materials (99·99% Zn, 99·99% Al, 99·99% Cu). The alloy was first melted in graphite crucible in a high temperature furnace, and then it was poured in a steel mold.

*Author for correspondence

The solution heat treatment at 350°C was performed on the ingots having cylindrical shape (70 mm diameter and 210 mm height). Chemical compositions of the alloy are given in table 1. In the first stage of experiment, acidic corrosion tests were conducted at room temperature using the conventional weight loss method according to the ASTM G69-80 Standards. The corroded specimen used was fresh 1 N HCl for 100 ml acidic per specimen. The samples were polished using SiC emery paper of grade 200–800 grit to obtain a smooth and identical surface. They were washed with water, followed by alcohol, and then were dried thoroughly. The cleaning procedures were used before each weighing at each stage of the corrosion test. Initially weighed specimens (14 mm diameter and 210 mm height) were immersed in the corrosive environment and taken out at 24 h intervals for testing up to a total of 384 h. Initially each weighed specimen was immersed in the corrosive environment once for different time duration 24, 48, 96, 192 and 384 h intervals as shown in figure 3. At each time corrosion product formed on the corroded specimens were removed by scrubbing the specimens with a bronze brush. The cleaned specimens were dried and weighed. The weight loss measurements were calculated and compared with the original weight of the uncorroded specimen. The specimens were weighed to an accuracy of three decimal places. The microstructure was examined with an Olympus optic microscopy (OM).

On the other hand, to study the corrosion depending on temperature, the specimens (4 mm diameter discs) taken from the polished samples were placed into an aluminum crucible in TGA-50 Schimadzu apparatus (heating rate of 10°C/min in atmospheric medium) which gives a proportional signal to the recorder and computer interface to plot the weight loss of alloy vs temperature. The results of curves were then evaluated.

Table 1. Chemical compositions of Zn-based alloys (wt.%).

Alloy	Zn	Al	Cu	Si	Sn
N1	73·58	24·32	1·0	0·082	0·40
N2	77·58	19·40	1·12	1·15	0·50
N3	72·47	23·90	1·10	2·40	0·523
N4	73·50	24·70	1·10	1·37	0·501

3. Results and discussion

3.1 *Microstructure and phase transformations*

The optical micrographs of the Zn-based alloys are shown in figures 1 and 2, where they correspond to temperature dependent and acidic medium of corrosion of the samples, respectively. In figure 2, it can be seen that several phases are formed in the microstructure of specimens. We note that the properties of elements of alloys and the literature involving similar studies may be useful to distinguish which phase was formed on OM pictures. Upon following this procedure, it can be seen that Zn–Al phases are main matrix ($a + b$ phase), and that Zn–Cu phase precipitations, AlO(Al_2O_3), ZnO oxides are formed between $a + b$ phase and grain boundaries and partially inside the grains (Boyer and Gall 1972; Showak and Dunbar 1972). Note that using the literature we can identify the dark regions appearing in the microstructure to be ZnO and AlO phases. Moreover, it appears that Si particles without being affected in solution and HCl medium have distributed in the main matrix. This can obviously be seen in figure 2 of N3 since Si content in N3 is the highest.

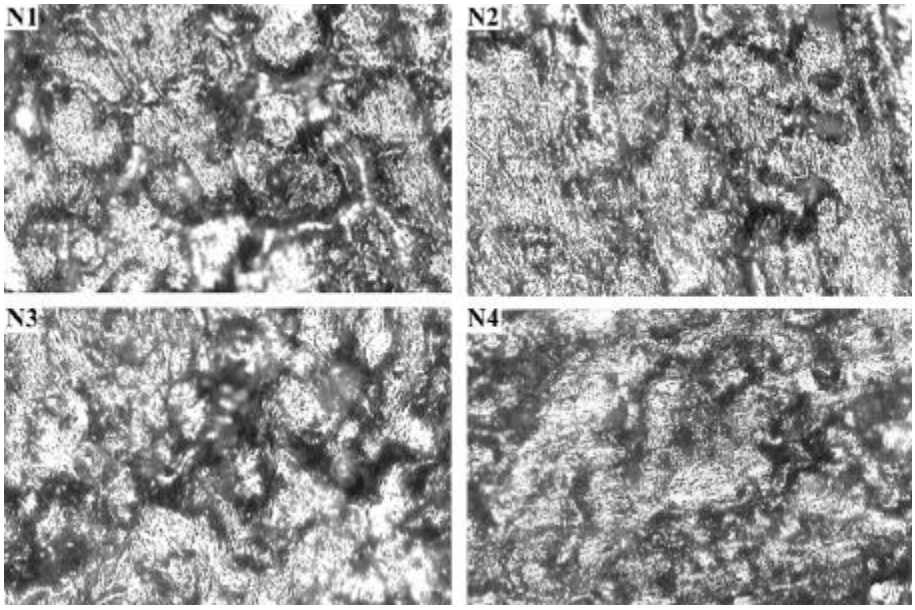

Figure 1. Optical micrographs of Zn-based alloys after corrosion (× 100) in TGA.

On the other hand, phase transformations have occurred in TGA process. As we look at the phase diagram in Toldin *et al* (1981), the results in figure 1 indicate that the phase structures up to 280°C have $a + b$ phase, $a + g$ phase at temperatures between 275 and 350°C, and a' at higher temperatures. In the figure it is also seen that the microstructure in a' phase transformed to $a + b$ phase at the end of slowly cooling from 450°C to room temperature. In particular, the alloy with ~77·5 wt.% Zn having a monotectoid reaction transformed from $a + b$ to a' phase at 275°C while the others remained in $a + g$ phase at the same temperature.

3.2 *Acidic corrosion behaviour*

To interpret the acidic corrosion, let us examine figure 3. It can be seen in the figure that the weight loss alters with exposure time. It appears that the weight loss initially increased, but then decreased as duration of time increased, and again an increase appeared with time, and so on. This altering situation continues with time in the acidic medium. Here it can be explained from this result that such changes is most probably due to presence of significant amount of Al in Zn main matrix since a stable Al-oxide layer forms on the surface of sample in HCl, which delays the dissolution of Zn phases (Fontana 1987; Li 2001). This argument is also remarked upon by Seah *et al* (1997). We also recall that Si content is not affected much in HCl solution.

3.3 *Temperature dependence of corrosion*

Figure 4 shows the weight loss on the surface of the samples as a function of time in which the corrosion took place on the surface of the specimens as a result of temperature applications from 50–500°C. The increase in the corrosion rate corresponding to weight loss appeared as

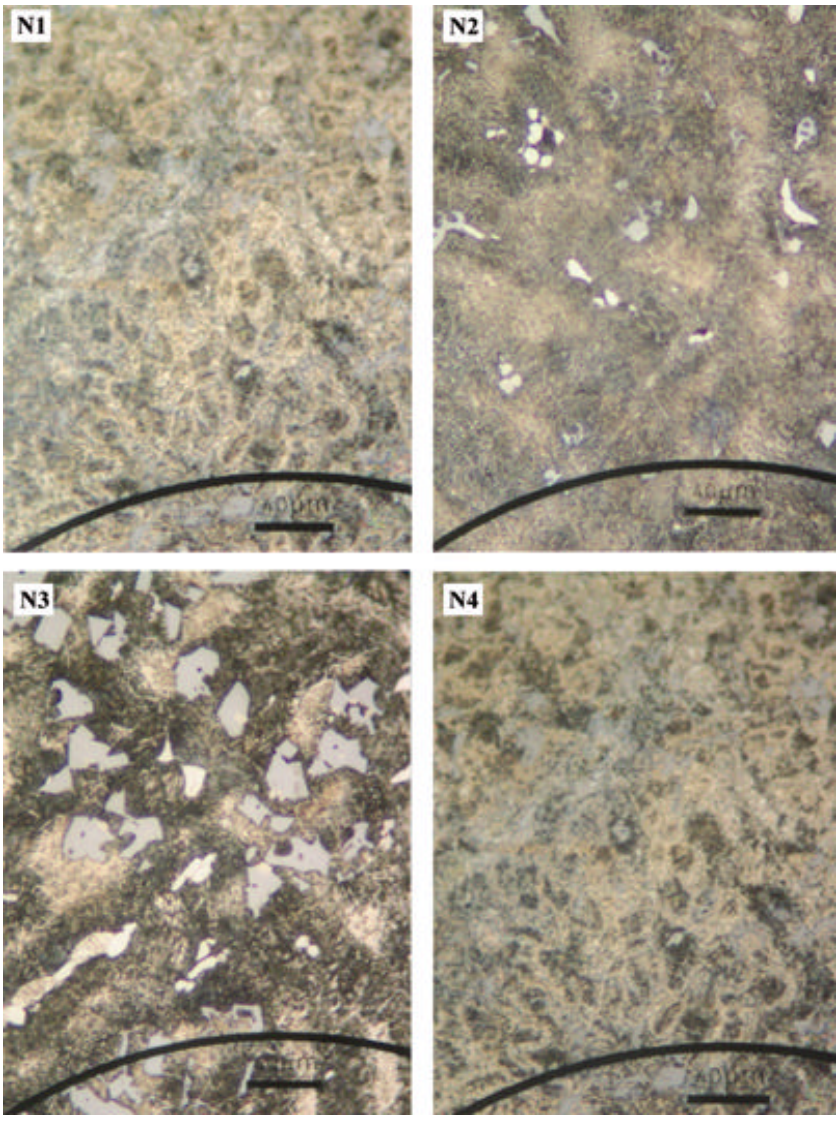

Figure 2. Optical micrographs of corroded Zn-based alloys in 1 N HCl solution.

structural changes on the surface of the specimens. We believe that this may be faster in evaporation of Zn no matter what Al contents are. Moreover, it is seen in the figure that similar behaviours, approximately, appear between the weight losses of all the samples.

In order to examine temperature dependence of corrosion, it is sometimes useful to calculate the corrosion parameter of alloys. To proceed in this direction, let us start with introducing the corrosion kinetic mechanism at a given temperature (Rishel *et al* 2002)

$$\Delta W = k_p t^{1/n}, \tag{1}$$

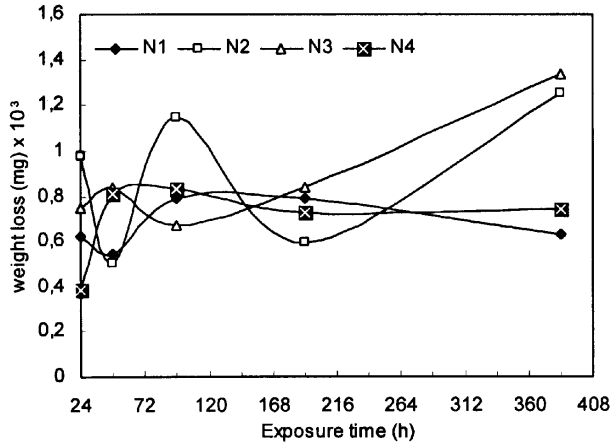

Figure 3. Graph of weight loss of Zn-based alloys vs exposure time in 1 N HCl solution.

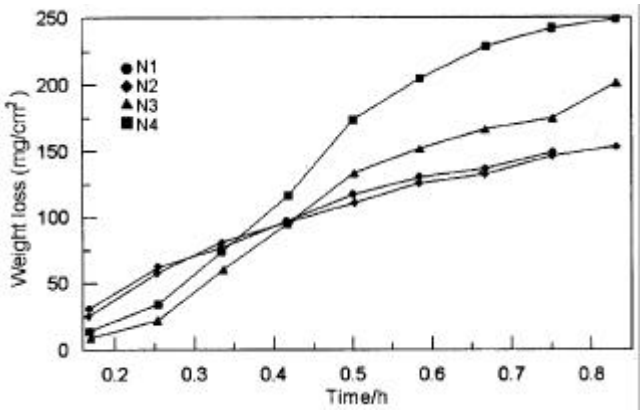

Figure 4. Graph of weight loss of Zn-based alloys vs time in TGA.

where ΔW is weight loss variation, k_p the corrosion rate, n a constant, and t the time of corrosion. The value of constants in (1) is determined from the logarithmic form of the equation, i.e.

$$\ln \Delta W = \ln k_p + 1/n \ln t. \tag{2}$$

Here it is evident that a plot of ΔW as a function of time, t, on logarithmic coordinates yields a straight line having a slope of $1/n$. The values of t were determined from the heating rate value of TGA (10°C/min). Then, the curves given in figure 4 were plotted as function of time. In order to obtain the value of n, figure 4 was plotted in logarithmic coordinates, in which two different regions corresponding to different n values occurred. Thus, two different n values, say n_1 and n_2, for each region were determined, and the best fitting values of the oxidation parameters are given in table 2. Moreover, the activation energy for corrosion behaviour can be determined from weight loss data. Variation of corrosion rate (k_p) with temperature is given by the following relation

$$k_p = k_0 \exp\left(-\frac{Q}{RT}\right), \tag{3}$$

where k_0 is the pre-exponential constant, Q the activation energy, R the gas constant and T the temperature. The numerical values of activation energies (Q_i) of corrosion behaviour were calculated from the slope of figure 5 for each region (regions I and II). The n values for each corrosion region showed that the corrosion process took place in two stages: reaction-controlled dissolution of the grain boundary phase and diffusion-controlled weight transport through the corrosion layer. k_0 in (3) gives a different meaning, i.e. k_R (reaction-controlled corrosion) and k_D (diffusion-controlled corrosion). The values of k_R and k_D were calculated from the intercept of curves of figure 5, which are given in table 2. Hence, the empirical expression corresponding to corrosion behaviour of the alloy studied can be defined in the following form

$$\Delta W(t) = k_R t + k_D \sqrt{t}. \tag{4}$$

A comparison in the activation energies of the alloys for first and second regions, respectively, was found as $Q_{N1} < Q_{N2} < Q_{N4} < Q_{N3}$, and $Q_{N1} < Q_{N2} < Q_{N3} < Q_{N4}$.

Table 2. Corrosion parameters of Zn-based alloys.

Alloy	Q_1 (kcal/mol)	Q_2 (kcal/mol)	k_D (mg cm^{-2} s^{-1})	k_R (mg cm^{-2} s^{-1})	n_1	n_2
N1	17·50	5·05	5·1 10^{-2}	2·42 10^{-3}	1·70	0·81
N2	25·35	5·31	0·37	2·07 10^{-3}	1·99	0·71
N3	45·23	6·77	80·47	1·74 10^{-2}	2·44	0·99
N4	38·49	7·51	10·10	1·34 10^{-2}	2·11	0·72

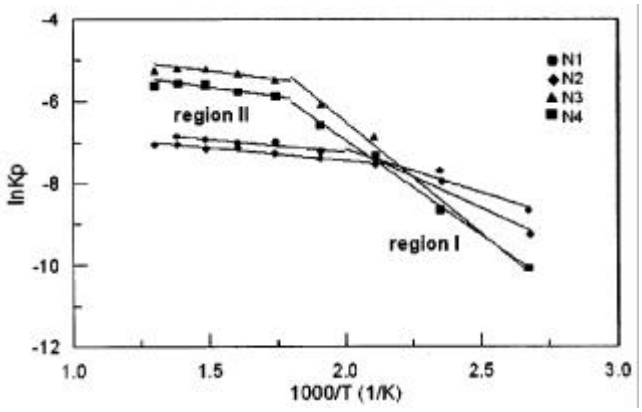

Figure 5. Graph of corrosion rate vs temperature of Zn-based alloys in TGA.

4. Conclusions

Zn-based alloys were studied for the purpose of investigating the corrosion behaviour both in 1N HCl solution and in temperature dependent TGA technique. The corrosion behaviour of Zn-based alloys did not show similarity in both mediums. In acidic medium, corrosion rate revealed an altering property by showing sometimes an increase and sometimes a decrease with time. This property was most probably due to presence of Al content. Moreover, Si content remained in the main matrix without being affected. On the other hand, an increase in the corrosion rate with increasing temperature was revealed in TGA. This property, most probably due to faster evaporation of Zn with temperature, led to both structural changes on the surfaces and phase transitions in microstructures of Zn-based alloys. The corroded microstructure results showed that $AlO(Al_2O_3)$, ZnO oxides and Zn–Cu phase precipitations were formed in main matrix, grain boundaries and partially inside the grains. The oxidation parameters and activation energies were also determined to reinforce the examination of corrosion variation with time in TGA. There exist some correlations between the parameter values of the samples. It might be intriguing to study these parameters in a separate study for alloys, which is under consideration for a future study.

Acknowledgements

This work is partially supported by Research Foundation of Firat University, contract grant-number: FUBAP 871.

References

Aylor D M and Moran P J 1985 *J. Electrochem. Soc.* **132** 1277

Boyer H E and Gall T L (eds) 1992 *Metals handbook* (Metals Park, Ohio: American Society for Metals) pp 6.64, 11.6 and 14.10

Colin S, Beche E, Berjoan R, Jolibois H and Chambaudet A 1999 *Corros. Sci.* **41** 1051

Dellis M A, Kaustermans J P, Delannay F and Wergra J 1991 *Mater. Sci. Eng.* **135** 253

Fontana M G 1987 *Corr. Eng.* (New York: McGraw-Hill) 3rd ed., p. 236

Li Y 2001 *Corr. Sci.* **43** 1793

Pohlman S L 1978 *Corrosion* **34** 156

Prasad B K 2000a *Mater. Charact.* **44** 301

Prasad B K 2000b *Mater. Sci. Eng.* **A277** 95

Rishel D M, Smee J D and Kammenzind B F 2002 *J. Nucl. Mater.* **303** 210

Seah K H W, Sharma S C and Girish B M 1997 *Corr. Sci.* **39** 1

Sharma S C, Seah K H W, Satish B M and Girish B M 1997 *Corr. Sci.* **39** 2143

Sharma S C, Somashekar D R and Satish B M 2001 *J. Mater. Process. Technol.* **118** 62

Showak W and Dunbar S R 1972 *Metals handbook*: *Atlas of microstructures of industrial alloys* (ed) T Leyman (Metals Park, Ohio: American Society for Metals) pp 339–340

Toldin V A, Burykin A A and Kleschev G V 1981 *Phys. Met. Metall.* **17** 116

Zhu Y H and Islas J J 1997 *J. Mater. Process. Technol.* **66** 244

Zhu Y H, Murphy S and Yeung C 1999 *J. Mater. Process. Technol.* **94** 78